Aerosol Science and Technology, 39:68–83, 2005

ISSN: 0278-6826 print / 1521-7388 online
DOI: 10.1080/027868290901963

Modification, Calibration and a Field Test of an Instrument for Measuring Light Absorption by Particles

Aki Virkkula,[1] Norman C. Ahlquist,[2] David S. Covert,[2] William P. Arnott,[3] Patrick J. Sheridan,[4] Patricia K. Quinn,[5] and Derek J. Coffman[5]

[1]*Finnish Meteorological Institute, Air Quality Research, Sahaajankatu, Helsinki, Finland*
[2]*Department of Atmospheric Sciences, University of Washington, Seattle, Washington, USA*
[3]*Desert Research Institute, Reno, Nevada, USA*
[4]*Climate Monitoring and Diagnostics Laboratory, National Oceanic and Atmospheric Administration, Boulder, Colorado, USA*
[5]*Pacific Marine Environmental Laboratory, National Oceanic and Atmospheric Administration, Seattle, Washington, USA*

A filter-based single-wavelength photometer (Particle Soot Absorption Photometer, PSAP) for measuring light absorption by aerosols was modified to measure at three wavelengths, 467 nm, 530 nm, and 660 nm. The modified and an unmodified photometer were calibrated during the Reno Aerosol Optics Study (RAOS) 2002 against two absorption standards: a photoacoustic instrument and the difference between the extinction and scattering coefficient. This filter-based absorption method has to be corrected for scattering aerosol and transmission changes. A simple function for this was derived from the calibration experiment as a function of transmission and single-scattering albedo. For an unmodified PSAP at typical atmospheric absorption coefficients the algorithm yields about 5–7% lower absorption coefficients than does the usually used method. The three-wavelength PSAP was used for atmospheric measurements both during RAOS and during the New England Air Quality Study (NEAQS).

INTRODUCTION

Single-scattering albedo (ω_0), the ratio of light scattering to light extinction by atmospheric particles is an important parameter when assessing the climatic effects of aerosols. The optical properties of aerosols depend on the wavelength of radiation. Scattering coefficient (σ_{SP}) is routinely measured using a 3-wavelength instrument but absorption coefficient (σ_{AP}) is usually measured at one wavelength and ω_0 at other wavelengths is calculated by assuming a λ^{-1} wavelength dependency of σ_{AP}. This may lead to errors in estimated aerosol radiative forcing because models need ω_0 as a function of wavelength (e.g., Heintzenberg et al. 1997; Bond 2001). In the visible wavelengths black carbon (BC) is usually the most important light absorbing aerosol component (e.g., Horvath 1993). The light absorption coefficient of small BC particles is approximately λ^{-1} over the visible band (e.g., van de Hulst 1957; Horvath 1993; Bergstrom et al. 2002). However, other absorbing species have different wavelength dependencies. For instance ferrous oxide, present in soil dust particles, has quite a different wavelength dependence (Lindberg et al. 1993) as do different types of coal combustion particles (Bond et al. 2002).

There are several methods for measuring absorption of light by aerosols. Descriptions and comparisons of methods are presented, e.g., by Clarke et al. (1987), Horvath (1993), Heintzenberg et al. (1997), and Reid et al. (1998). Real-time measurements of light absorption by aerosols are mainly done using two filter-based instruments, the aethalometer® (Hansen et al. 1984; Magee Scientific) and the Particle Soot Absorption Photometer (PSAP, Radiance Research, Seattle, WA). They are both improved versions of the Integrating Plate (IP; Lin et al. 1973) method. Recently a new continuous filter-based method has been presented, the Multi-Angle Absorption Photometer (Petzold et al. 2002, 2005; Petzold and Schönlinner 2004; MAAP, Andersen Instruments).

Filter-based methods are easy to use, relatively inexpensive and suitable for unattended use. However, they have to be

Received 26 January 2004; accepted 22 October 2004.

The RAOS experiment was supported by the U.S. Department of Energy Atmospheric Radiation Measurement (ARM) Program and the NOAA Aerosol-Climate Interactions Program. The lead author was supported by postdoctoral grants from the National Research Council, the Vilho, Yrjö, and Kalle Väisälä Foundation (Finland), and the 100th Anniversary Foundation of Helsingin Sanomat (Finland).

Address correspondence to Aki O. Virkkula, Air Quality Research, Finnish Meteorological Institute, Sahaajankatu 20E, 00880 Helsinki, Finland. E-mail: aki.virkkula@fmi.fi

calibrated using some direct, absolute method for measuring light absorption. The most direct method for doing this is measuring the difference between extinction and scattering coefficient (coefficients (e.g., Gerber 1982; Horvath 1993; Heintzenberg et al. 1997). This has been used as the absorption standard by Horvath (1997) who calibrated the IP; Bond et al. (1999), who calibrated the PSAP; and most recently by Weingartner et al. (2003), who calibrated the aethalometer during the Aerosols: Interaction and Dynamics in the Atmosphere (AIDA) soot characterization campaign in 1999. Arnott et al. (2005) have evaluated aethalometer data from RAOS using a two-stream radiative transfer model for the multiple scattering enhancement that occurs for particles on filters. A compact analytical approximation was obtained for the effects of both filter loading and the offset due to scattering aerosol. The approximate model is not directly applicable to the PSAP because the optical transmission through filters used for the PSAP is more than double that of filters used on the aethalometer, and the spectral dependence is much greater for the PSAP.

Until now, the PSAP has only been available in one wavelength. This article discusses the modification of the PSAP so that it measures light absorption at three wavelengths close to those of the three-wavelength nephelometer (TSI model 3563, St Paul, MN, USA). Several prototypfe three-wavelength PSAPs have since been made at the University of Washington and are available commercially. A modified PSAP and an unmodified single-wavelength PSAP were calibrated during the Reno Aerosol Optics Study 2002 (RAOS 2002). The objectives of the campaign were to characterize new and existing instruments for measuring aerosol light absorption and extinction, quantify the uncertainty in the measurements of aerosol light-absorption coefficient, and derive methods for determining spectral aerosol absorption from multiwavelength measurements of absorption. At RAOS two absorption standards were used: (1) the difference between extinction and scattering coefficient, measured with an optical extinction cell and an integrating nephelometer; and (2) absorption measured using a photoacoustic instrument (Arnott et al. 1999). Results from RAOS are presented also in companion papers by Sheridan et al. (2005), Petzold et al. (2005), and Virkkula et al. (2005).

The goal of this article is to present the three-wavelength modification of the PSAP and analyze its performance in real atmospheric aerosol measurements. Basic principles of filter-based absorption measurements are presented first. Next, some technical details of the PSAP modification are discussed, and then data from the RAOS calibration experiment. The calibration experiment data are used for deriving empirical formulas for calculating absorption coefficient from the PSAP raw data. Using these formulas, the wavelength dependency of absorption coefficient of both laboratory-generated and real atmospheric aerosols is calculated. The modified PSAP was used for measuring real atmospheric aerosols first during RAOS and then during the New England Air Quality Study (NEAQS). The symbols used in the paper are presented in Table 1.

BASIC FORMULAS

A filter-based absorption measurement can be made by drawing air through a filter and measuring the decrease of light transmission through the sampling area (e.g., Lin et al. 1973). In principle the absorption coefficient for such a method can be derived (e.g., Weingartner et al. 2003) from the Beer-Lambert law as

$$\sigma_0 = \frac{A}{V}\ln\left(\frac{I_{t-\Delta t}}{I_t}\right), \quad [1]$$

where A is the area of the sample spot, V is the volume of air drawn through the spot area during a given time period Δt, and $I_{t-\Delta t}$ and I_t are the filter transmittances before and after the time period. This is the principle of both the aethalometer and the PSAP. However, Equation (1) does not give the absorption coefficient directly because of various inherent error sources. Both scattering and absorbing particles collected on the filter alter the internal reflection of the filter in a way that increases the absorption of the aerosol/filter combination (Clarke 1982; Clarke et al. 1987; Petzold et al. 1997; Horvath 1997; Bond et al. 1999). There are several methods for handling these effects see references by Bond et al. (1999) and Weingartner et al. (2003). Lindberg et al. (1999) investigated this problem theoretically using the Kubelka-Munk theory and showed that light attenuation through a filter sample is a function of scattering and absorption properties of the particle layer and the reflectance of the filter. In the MAAP this problem is solved by measuring the decrease of transmission and also light scattering from the aerosol-filter system. The data evaluation algorithm includes multiple-scattering effects into the analysis of the aerosol-filter system (Petzold et al. 2002, 2005).

In calibrating the modified PSAP, the approach by Bond et al. (1999) was followed to determine the correction factors. The approach is strictly empirical; no scattering theory is used. First, the relationship between the true absorption coefficient and transmission decrease changes as the filter gets darker. This relationship is taken into account by the transmission correction function f(Tr). Second, the presence of purely white, light-scattering aerosol also decreases transmission through the filter. Without any information on the scattering coefficient, σ_{SP}, in the sample air this effect would be interpreted as absorption (called the *apparent absorption* in the rest of the work). The apparent absorption will be corrected by subtracting a fraction of the scattering coefficient from the absorption coefficient. This fraction is determined in the calibration, and it is called the scattering correction factor, s. Taking these two factors into account, the absorption coefficient may be calculated from

$$\sigma_{AP} = f(Tr)\sigma_0 - s \cdot \sigma_{SP}. \quad [2]$$

Bond et al. (1999) discussed both f(Tr) and s for an unmodified single-wavelength PSAP. In this work the f(Tr) and s will be derived both for the three-wavelength PSAP and a single-wavelength PSAP. In the rest of the work the absorption coefficient calculated using Equation (2) will be written as

Table 1
Nomenclature

Symbol	Definition	Unit	Equation
A	Sample spot area	cm^{-2}	1
α_{12}	Ångström exponent of either absorption or scattering coefficient at wavelengths λ_1 and λ_2	—	
α_{AP}	Ångström exponent of absorption coefficient	—	
α_{AP}(AP)	Ångström exponent of σ_{AP}(PA)	—	
α_{AP}(PSAP)	Ångström exponent of σ_{AP}(PSAP)	—	
α_{AP}(Ref)	Ångström exponent of σ_{AP}(Ref)	—	
α_{SP}	Ångström exponent of scattering coefficient	—	
$\alpha(\omega_0)$	Ångström exponent of single-scattering albedo		
f(Tr)	Transmission correction function for σ_0	—	2, 5, 8
f_M(Tr)	Measured transmission correction function for σ_0	—	6
h(ω_0)	Single-scattering correction function of f(Tr)	—	
h_0 and h_1	Constants in h(ω_0)	—	7
I_t	Filter transmittance at time t	—	1
k_0 and k_1	Constants in f(Tr)	—	7
ω_0	Single-scattering albedo = $\sigma_{SP}/(\sigma_{AP} + \sigma_{SP})$	—	
Ref	Output of reference detector of the PSAP	Counts	3
σ_0	Uncorrected absorption coefficient	Mm^{-1}	1, 4
σ_1, σ_2 and σ_x	Either absorption or scattering coefficient, used for presenting the logarithmic interpolation	Mm^{-1}	
σ_{AP}	Absorption coefficient	Mm^{-1}	
σ_{PSAP}	Absorption coefficient calculated from the PSAP before the scattering correction	Mm^{-1}	4
σ_{AP}(PSAP)	Absorption coefficient calculated from σ_{PSAP}, including the scattering correction	Mm^{-1}	2, 7, 9
σ_{AP}(PA)	Absorption coefficient, photoacoustic instrument	Mm^{-1}	
σ_{AP}(ref)	Absorption coefficient, reference absorption	Mm^{-1}	
σ_{EP}	Extinction coefficient, optical extinction cell	Mm^{-1}	
σ_{SP}	Scattering coefficient	Mm^{-1}	
s	Scattering correction factor	—	
Sig	Output of signal detector of the PSAP	Counts	3
Tr	Transmission of light through the filter	—	3
V	Volume of air drawn through spot area A	m^3	1

σ_{AP}(PSAP), and the absorption coefficient obtained from the absorption standards will be written as σ_{AP}.

PSAP MODIFICATION

Hardware Modifications

A schematic picture of the single-wavelength PSAP was presented by Bond et al. (1999). The main modifications of this instrument consist of (1) replacing the original green LED with blue, green, and red LEDs; (2) replacing the light source block; (3) replacing the light detectors; and (4) adding a control circuit that switches the LEDs on and off in a cycle.

Figure 1 shows details of the three-wavelength PSAP light source block. The light source is a 55 mm high and 25 mm diameter aluminum cylinder. At the top of the cylinder, three LEDs are attached in a row. The blue LED is in the middle and the higher intensity red LED is placed to the side in order to get the signal levels more or less within the same range. The blue, green, and red LEDs were AND520HB, AND520HG, and AND180CRP, respectively (AND® Purdy Electronics, Sunnyvale, CA, USA). Both signal and reference detectors were changed so that they would respond better to the full wavelength range. The new detectors were silicon photodiodes (Hamamatsu, S2387-66R) that have an active area size 5.8 mm × 5.8 mm.

The effective wavelength of the LED-photodiode detector combination was measured at University of Washington using a Beckman model-B spectrophotometer calibrated to Hg lines and a HeNe laser. The detector-weighted average wavelengths were determined to be 467 nm, 530 nm, and 660 nm, respectively (Virkkula et al. 2005). The effective wavelength of an unmodified PSAP was also measured at UW using the same procedure as for the three-wavelength PSAP. It was determined to be 574 nm, and this wavelength will be used in the rest of this article. The effective wavelength of the unmodified PSAP used at RAOS is assumed to be the same 574 nm as for unit that was measured at UW.

Below the LEDs there are two 25 mm holographic diffusers (Edmund Industrial Optics; HD1, circular diffusing angle 25°;

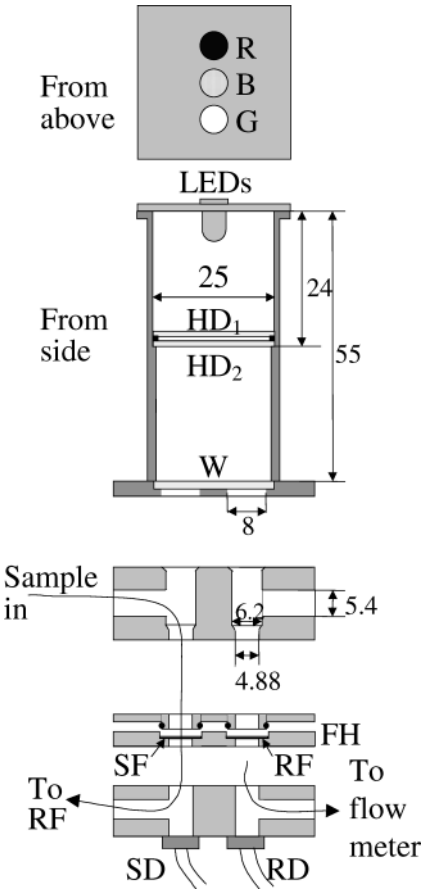

Figure 1. Schematics of the light source, filter, and detector blocks of the 3λPSAP. R, B, and G, LEDs (λ = 660 nm, 467 nm, and 530 nm, respectively); HD, holographic diffuser; W, window; FH, filter holder; SF, sample filter; RF, reference filter; SD, signal detector; RD, reference detector. Dimensions are in mm.

HD2, elliptical diffusing angle $5^\circ \times 30^\circ$). The purpose of the diffusers is to spread the light as uniformly as possible over the two light path apertures. At the bottom of the light source block there is an antireflection coated window (Edmund Industrial Optics, B270, 25 mm diameter, 2 mm thick, 1/4 wave MgF_2). The purpose of the window is to seal the light source block from the sample air path. The transmission or these windows is greater than 90% from 200 nm to 6 μm.

Software

An external program sent signals to the SSRs to switch the LEDs on and off. The program cycles the LEDs with a user-defined cycle time, minimum 6 s. The output of the PSAP was read through a serial port. The program used time, flow, signal, and reference detector outputs of the original PSAP. The transmission and absorption coefficient data calculated in the PSAP firmware were not used.

The purpose of the reference detector is to account for variations in light intensity, and the calculation of filter transmission is based on the decrease of the signal-to-reference detector ratio over time. Transmission depends on wavelength, and it has to be calculated separately for each wavelength from the raw data as:

$$\mathrm{Tr} = \frac{\left(\sum \mathrm{SIG}/\sum \mathrm{REF}\right)}{\left(\sum \mathrm{SIG}/\sum \mathrm{REF}\right)_{t=0}}, \quad [3]$$

where ΣSIG and ΣREF are the sums of Signal and Reference detector outputs during the summing period, and time t = 0 is the time of changing the filter. $(\Sigma\mathrm{SIG})_{t=0}$ and $(\Sigma\mathrm{REF})_{t=0}$ are the sums of the signal and reference detector output after the summing period that started at t = 0, and $(\Sigma\mathrm{SIG})_t$ and $(\Sigma\mathrm{REF})_t$ are the sums of the signal and reference detector outputs after the summing period that started at time t. Next the program calculates the absorption coefficient from

$$\sigma_{\mathrm{PSAP}} = \mathrm{f(Tr)}\frac{\mathrm{A}}{\mathrm{Q}\Delta t}\ln\left(\frac{\left(\sum \mathrm{SIG}/\sum \mathrm{REF}\right)_{t-\Delta t}}{\left(\sum \mathrm{SIG}/\sum \mathrm{REF}\right)_{t}}\right) = \mathrm{f(Tr)}\sigma_0, \quad [4]$$

where Δt is the summing period. For instance, if Δt = 6 s is the total cycle time, time resolution is 18 s. However, the first second of the data was always discarded because heating the LED to a stable intensity and wavelength takes time. So, actually for the 18 s cycle time the sums included 5 s of data. The transmission correction function in the firmware of the unmodified PSAP (Bond et al. 1999) is

$$\mathrm{f(Tr)} = \frac{1}{1.0796 \cdot \mathrm{Tr} + 0.71}. \quad [5]$$

This was used in the software for all wavelengths as a first approximation to facilitate comparison of the modified PSAP with the unmodified one-wavelength PSAP during the calibration experiments. According to the calibration of Bond et al. (1999) the f(Tr) presented in Equation (5) should further be multiplied by a spot size correction factor and divided by a calibration constant. For details see Bond et al. (1999) and Sheridan et al. (2005).

Spot Sizes

Two PSAPs were calibrated against the standards, the three-wavelength PSAP (3λPSAP) and an unmodified PSAP. The spot diameters (cf. Equation (1)) of both PSAPs were measured using the same procedure. Four people each did 10 measurements of three filters sampled with the PSAPs using an ocular eyepiece. The average of the 3λPSAP spot diameters was 4.92 mm, and the average of unmodified 1λPSAP spot diameters was 5.017 mm. The ratio of the largest to smallest average spot diameter for each of the three filters varied between 1.035 to 1.043. This means that the four people got an approximately 4% agreement on the diameter, yielding an 8% uncertainty in the spot area, and thus the resulting absorption coefficient without independent calibration.

Noise Test

The instrumental noise of the 3λPSAP was measured by sampling filtered, particle-free air. The absorption coefficient was

Table 2
Noise of 1 min averaged absorption coefficient as a function of LED cycle time from the 3λPSAP before scattering correction

	467 nm		530 nm		660 nm	
Cycle time	Std.	Max–min	Std	Max–min	Std	Max–min
6	0.79	3.6	0.47	2.1	0.58	2.7
9	0.58	2.3	0.18	0.7	0.15	0.6
15	0.58	4.2	0.14	0.7	0.13	1.1
30	0.53	4.7	0.16	1.5	0.15	1.7
60	0.36	1.4	0.10	0.4	0.07	0.2

For details see text. Unit: Mm^{-1}.

calculated before scattering correction, i.e., using Equation (4). The cycling time of the LEDs was set to 6, 9, 15, 30, and 60 s. The cycling time was kept constant for a period of 30 min, then changed. When the cycling time was set to 60 s the filtered-air period was set to 60 min. The data were averaged for 1 min periods, and the standard deviation and the peak-to-peak difference over the period was calculated. The results are presented in Table 2. For instance, when the cycling time was set to 6 sec, the standard deviation of 1-min-averaged absorption coefficients at 530 nm was 0.5 Mm^{-1} and the peak-to-peak difference 2.1 Mm^{-1}. The noise is reduced when the cycling time is increased, the lowest noise was observed when the cycling time was set to 60 s. The blue LED was the noisiest, the red the most stable. The noise of the absorption coefficient calculated from Equation (2) is higher than those in Table 2 because of the scattering correction that introduces noise of the scattering coefficient to the data.

PSAP CALIBRATION

During the RAOS 2002, absorbing and scattering aerosols were produced at several concentrations and delivered to all measurement instruments. The setup and the experiments are discussed in detail in a companion article by Sheridan et al. (2005). The absorbing aerosols used were soot from a kerosene lamp, graphite from a carbon vane pump, and soot from a diesel generator. The scattering particles were ammonium sulfate produced using an ultrasonic nebulizer and polystyrene latex spheres. In the following text, the RAOS test aerosols that were nonabsorbing, i.e., ammonium sulfate (AS) and polystyrene latex, will be called *white*, the kerosene soot aerosols will be called *black*, and the mixtures of white and black aerosols will be called *grey*. The data from the experiments where black aerosol was produced with carbon vane pump and diesel generator are not used in this work.

Absorption Standards

At RAOS two absorption standards were used: the photoacoustic method (PA) that measures absorption at 532 and 1047 nm (Arnott et al. 1999, 2003), and the difference between extinction coefficient and scattering coefficient ($\sigma_{AP} = \sigma_{EP} - \sigma_{SP}$). The extinction coefficient was measured using an optical extinction cell (OEC) (Virkkula et al. 2005) that measures at the same wavelengths as the 3λPSAP. The scattering coefficient was measured using a TSI three-wavelength nephelometer (Model 3653 TSI, St. Paul, MN, USA) that measures at 450 nm, 550 nm, and 700 nm.

The absorption coefficients from the PA and the scattering coefficients from the nephelometer were interpolated to the LED wavelengths λ_x according to $\sigma_x = \sigma_1(\lambda_1/\lambda_x)^{\alpha_{12}}$, assuming a constant Ångström exponent $\alpha_{12} = -\log(\sigma_1/\sigma_2)/\log(\lambda_1/\lambda_2)$ between wavelengths λ_1 and λ_2 and extrapolated assuming it stays the same also beyond these wavelengths. The uncertainty due to this assumption can be estimated from the two absorption standards. In general the Ångström exponent of the absorption coefficient calculated from the difference method, $\alpha_{AP}(\sigma_{EP} - \sigma_{SP})$ was slightly smaller than that calculated from the PA data α_{AP}(PA) (Virkkula et al. 2005). For instance, in the highly absorbing range ($\sigma_{AP} > 300$ Mm^{-1}) the average $\alpha_{AP}(\sigma_{EP} - \sigma_{SP})$ between the wavelengths 467 and 660 nm was 0.98, and the average α_{AP}(PA) was 1.12. The noise of the 1 min α_{AP}(PA) data was ∼0.03 in the range $\sigma_{AP} > 300$ Mm^{-1}, ∼0.4 in the range 5–20 Mm^{-1}, and ∼1.4 in the range < 5 Mm^{-1}. The noise of the $\alpha_{AP}(\sigma_{EP} - \sigma_{SP})$ was much higher in the less-absorbing ranges. The uncertainty of σ_x due to uncertainty in α_{12} can be estimated from $\delta\sigma_x = |\sigma_1(\lambda_1/\lambda_x)^{\alpha_{12}} \ln(\lambda_1/\lambda_x)|\delta\alpha_{12} \Leftrightarrow \delta\sigma_x/\sigma_x = |\ln(\lambda_1/\lambda_x)|\delta\alpha_{12}$. The average α_{AP} was ∼1.0 ± 0.2. When extrapolating σ_{AP} from 532 to 467 nm, the uncertainties of α_{AP} thus result in σ_{AP} uncertainties of ∼1.5% in the range $\sigma_{AP} >$ 300 Mm^{-1}, ∼6% in the range 5–20 Mm^{-1}, and ∼20% in the range < 5 Mm^{-1}. The overall uncertainties are higher, but these figures are only those due to the uncertainty of α_{AP}.

The noise of the absorption coefficient calculated as the standard deviation of $(\sigma_{EP} - \sigma_{SP})$ from 1 min averaged white aerosol data was about 10, 11, and 5 Mm^{-1} for the blue, green, and red wavelengths, respectively (Virkkula et al. 2005). The performance of the PA was discussed by Arnott et al. (1999). The broadband acoustic and electronic noise of the PA is 0.4 Mm^{-1} at 8 min averaging time when using a laser power 60 mW (Arnott et al. 1999). The noise of the PA varies inversely with laser power and inversely with the square root of the averaging time. At RAOS the PA laser power was 35 mW. Using the above relationships yields a noise level of approximately 1.9 Mm^{-1} for the PA at the 1 min averaging time used in the present work.

In general the two methods agreed well, within ∼3–7%, depending on wavelength (Virkkula et al. 2005). Since there was no way of knowing a priori which of these two methods is better, it was decided to use the average of the photoacoustic measurement and the difference method as the reference absorption coefficient against which to calibrate the PSAP. The absorption standard measurement methods are discussed more in companion articles (Sheridan et al. 2005; Virkkula et al. 2005).

EMPIRICAL TRANSMISSION CORRECTION FUNCTION

As a first approximation the formulas obtained by Bond et al. (1999) were used for all PSAP measurements. The results show that these formulas work fairly well; the regression lines are close to the 1:1 line, especially for the nonmodified PSAP in the low absorption range (Figure 2). In principle a simple slope-and-offset correction might be enough for a calibration of both the 1λPSAP and the 3λPSAP. However, there are clear deviations. For the 3λPSAP all grey aerosol data points are above the 1:1 line, whereas most black aerosol data are below the line. For the

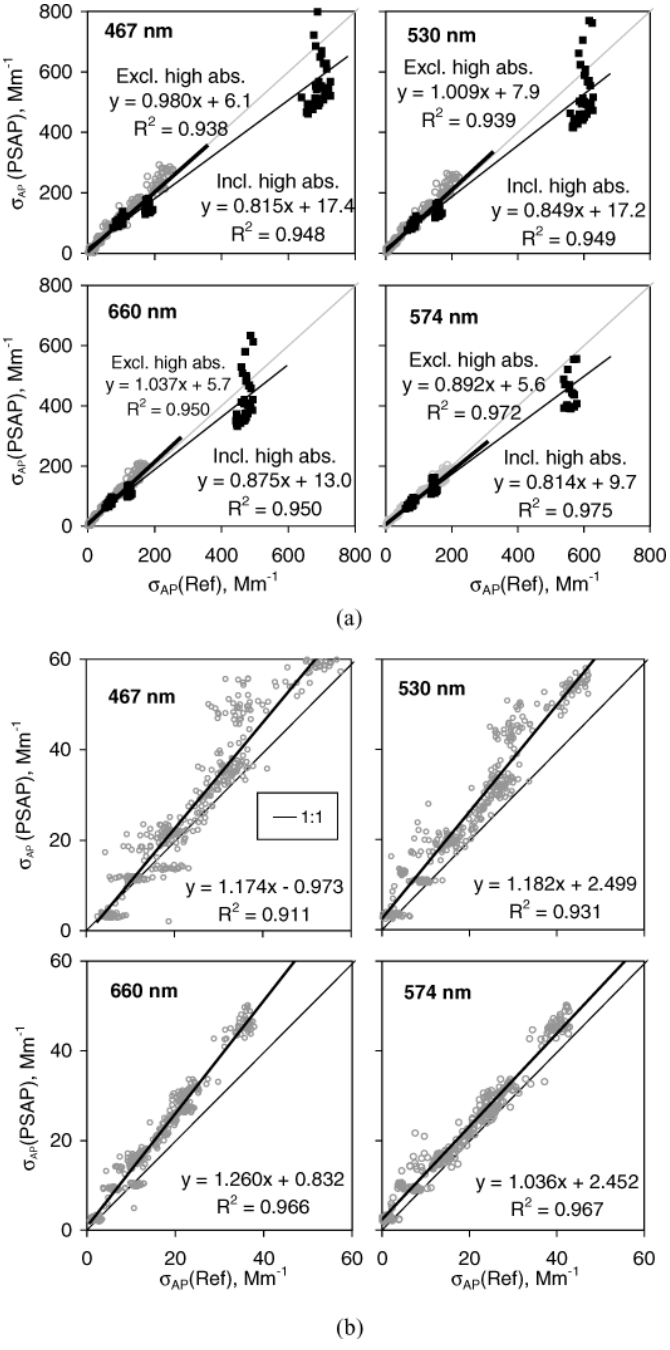

Figure 2. Comparison of absorption coefficients from the PSAPs using the Bond et al. (1999) formula for all wavelengths and the absorption standard. The regression lines were fitted using 1 min for (a) all grey and black experiments data, including and excluding the most absorbing experiment, (b) experiments with $\sigma_{AP}(467\ nm) < 60\ Mm^{-1}$.

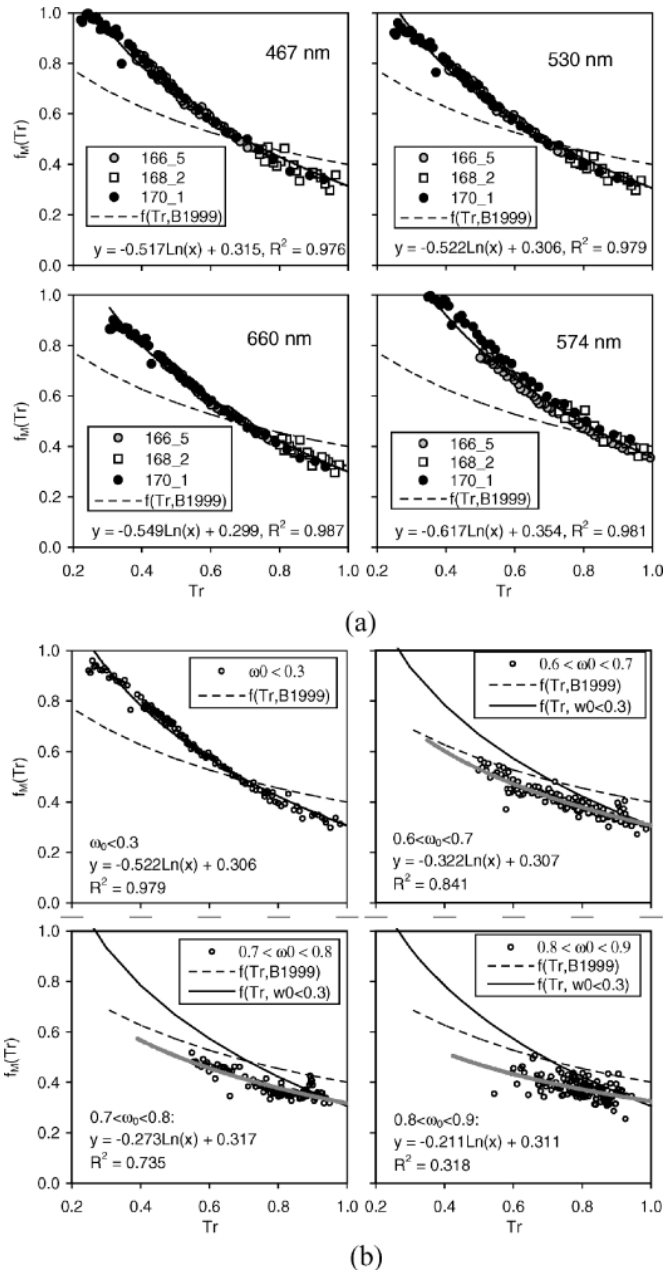

Figure 3. Measured transmission correction function $f_M(Tr)$. f(Tr,B1999) is shown for comparison in all graphs. (a) Black experiments, all wavelengths. 166_5, 168_2, 170_1: different black aerosol experiments (details in text), curve fit using all three experiments' data. (b) 530 nm data at four ω_o intervals. In the higher ω_o ranges also f(Tr, black) is shown for comparison.

1λPSAP, the grey aerosol data are close to the 1:1 line but the black aerosol data below are the line. An explanation for these observations is required.

Since a reference absorption coefficient σ_{AP} was available, the transmission correction function was calculated from Equation (2). This is the measured transmission correction function:

$$f_M(Tr) = \frac{\sigma_{AP} + s \cdot \sigma_{SP}}{\sigma_0}. \quad [6]$$

It is plotted against Tr for the 3λPSAP λ = 530 nm in Figure 3. Also, the transmission function of the PSAP firmware (Equation (5)), multiplied by the correction factors obtained by Bond et al. (1999), is plotted in Figure 3 for comparison. This function is referred to as f(Tr, B1999). For the grey aerosols $f_M(Tr) < f(Tr,B1999)$, and for low ω_0 they intersect at one point, which explains the black aerosol points in Figure 2 that fall on the 1:1 line.

The shape of the plots is similar for all wavelengths. A logarithmic function $f(Tr) = k_0 + k_1 \ln(Tr)$ fits the black aerosol data well (Figure 3a), and $\sigma_{AP}(PSAP)$ can be calculated from

$$\sigma_{AP}(PSAP) = (k_0 + k_1 \ln(Tr))\sigma_0 - s\sigma_{SP}. \quad [7]$$

There were three experiments with black aerosol (experiment codes 166_5, 168_2, and 170_1). The average reference absorption coefficient (λ = 530 nm) in these experiments was 159 Mm^{-1}, 83 Mm^{-1}, and 596 Mm^{-1}, respectively, and still all the $f_M(Tr)$ points follow the same line (Figure 3a). This suggests that the f(Tr) is independent of absorption coefficient. The values for k_0, k_1, and s were obtained by an iterative procedure. First, the value obtained by Bond et al. (1999) for the scattering correction factor s was used, and the two constants k_0 and k_1 were fit using the black aerosol data. Then, using the obtained f(Tr), a new value for s was found by fitting to the ammonium sulfate experiments. These steps were repeated as long as k_0, k_1, and s changed. The values converged after two or three iterations. Finally, the 95% confidence intervals for k_0 and k_1 were obtained from by noting that f(Tr) can be linearized to $k_0 + k_1 X$. The confidence intervals can be obtained for the slope and offset based on T distribution. The linear regression was done both for all wavelengths separately and for all three wavelengths of the 3λPSAP together. The 1λPSAP regressions were done separately. The results are presented in Table 3. The constants k_0 and k_1 for 467 nm and 530 nm are not significantly different. The 660 nm k_1 constant is most clearly outside the 95% confidence interval obtained from the fit to all three wavelength data. The 1λPSAP k_0 and k_1 constants are significantly different from those obtained for the 3λPSAP.

For grey aerosols, $f_M(Tr)$ clearly deviates from that of the black aerosols (Figure 3). To find a relationship between f(Tr) and the darkness of the aerosol, the data were classified according to single-scattering albedo ω_0, and the same type of function was fit again. For the aerosols with $\omega_0 < 0.9$, a logarithmic f(Tr) fits well, but with increasing ω_0 the correlation coefficient decreases (Figure 3b). For grey aerosols at $\omega_0 > 0.9$ there is no clear correlation, which is due to a small denominator (σ_0) and noise at low σ_{AP} in Equation (6).

Two important observations can be made from the logarithmic curves (Figure 3b): factor k_0 remains close to constant but k_1 decreases with increasing ω_0, and the relationship between k_1 and ω_0 is linear (Figure 4). Thus, a new form for the transmission correction function can be written:

$$f(Tr, \omega_0) = k_0 + k_1 h(\omega_0) = k_0 + k_1(h_0 + h_1\omega_0), \quad [8]$$

and absorption coefficient is then calculated from

$$\sigma_{AP}(PSAP) = (k_0 + k_1 h(\omega_0)\ln(Tr))\sigma_0 - s\sigma_{SP}. \quad [9]$$

A 95% confidence interval was calculated for the constants k_0 and k_1 and also for the constants h_0 and h_1 (Table 3). For the scattering correction factors, s(λ), a range is given in Table 3. The procedure for obtaining the range will be discussed below.

There is a problem in Equation (9); in order to calculate the absorption coefficient, the single-scattering albedo has to be known, and for that the absorption coefficient has to be known. This can be solved by a simple procedure:

1. Calculate $\sigma_{AP}(PSAP)$ using Equation (7).
2. Calculate an estimate of ω_0 using this absorption coefficient.

Table 3
Constants for the equation $\sigma_{AP}(PSAP) = (k_0 + k_1(h_0 + h_1\omega_0)\ln(Tr))\sigma_0 - s\sigma_{SP}$.

	3λPSAP				1λPSAP
	467 nm	530 nm	660 nm	Fit to all 3λPSAP data	574 nm
$k_0 \pm$ c.l.	0.315 ± 0.011	0.306 ± 0.010	0.299 ± 0.007	0.308 ± 0.005	0.354 ± 0.009
$k_1 \pm$ c.l.	−0.517 ± 0.015	−0.522 ± 0.014	−0.549 ± 0.012	−0.526 ± 0.008	−0.617 ± 0.016
$h_0 \pm$ c.l.	1.212 ± 0.198	1.234 ± 0.078	1.161 ± 0.049	1.207 ± 0.062	1.192 ± 0.219
$h_1 \pm$ c.l.	−0.860 ± 0.289	−0.952 ± 0.116	−0.748 ± 0.082	−0.864 ± 0.095	−0.800 ± 0.336
s (min, max)	0.013 (0.009, 0.020)	0.016 (0.011, 0.023)	0.021 (0.016, 0.029)	0.017 (0.009, 0.029)	0.023 (0.017, 0.031)

The fitting was done using the average of σ_{AP}(PA) and $\sigma_{AP}(\sigma_{EP} - \sigma_{SP})$ as the absorption standard.
For k_0, k_1, h_0, and h_1, the errors are the 95% confidence limits.
For the scattering correction factors s a range is given, calculation described in text.

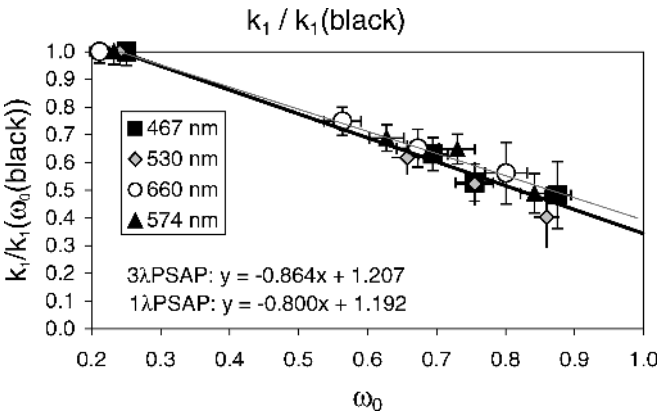

Figure 4. Variation of k_1 as a function of single-scattering albedo.

3. Calculate σ_{AP}(PSAP) using Equation (9).
4. Repeat (2) and (3) until σ_{AP}(PSAP) does not change significantly.

The convergence depends on Tr and ω_0. Using the values presented in Table 3, it can be shown that at Tr > 0.5 and $\omega_0 > 0.3$ the algorithm converges and at usual atmospheric conditions already after the first iteration. For instance, assume that at $\lambda =$ 530 nm $\sigma_{SP} = 100$ Mm^{-1}, $\sigma_0 = 50$ Mm^{-1}, and Tr = 0.8. After procedure steps (1) and (3), σ_{AP}(PSAP) = 19.42 Mm^{-1} and 16.56 Mm^{-1}, respectively. Repeating steps (2) and (3) yields σ_{AP}(PSAP) = 16.46 Mm^{-1}, a change of ~0.6%.

The RAOS PSAP data were processed using this algorithm. After one iteration most data points moved close to the 1:1 line, and linear regressions yielded slopes close to one for all wavelengths (Figure 5). For the 3λPSAP the average $h_0 = 1.21$ and $h_1 = -0.86$ (Table 3) were used for all three wavelengths in Equation (9) since it yielded somewhat better regression lines than the wavelength-dependent factors. For instance, with the h_0 and h_1 values for 530 nm σ_{AP}(PSAP) = $0.96\sigma_{AP}$(ref) + 1.02 instead of $0.97\sigma_{AP}$(ref) + 1.03 at absorption coefficient range < 60 Mm^{-1} (Figure 5b). For 467 and 660 nm the change was even smaller. For the 1λPSAP, the values presented in Table 4 were used. If the 3λPSAP values $h_0 = 1.21$ and $h_1 = -0.86$ were used for the 1λPSAP, the regression line becomes σ_{AP}(PSAP) = 0.965 σ_{AP}(ref) + 1.164 Mm^{-1} instead of σ_{AP}(PSAP) = 0.977 σ_{AP}(ref) + 1.164 Mm^{-1} shown in Figure 5b.

The remaining deviations from the 1:1 line are now more probably due to noise in the reference absorption than in the PSAP. For an example of this, data from three experiments, 165_1A, 168_5, and 172_6 are highlighted in Figure 5b for 467 nm. The PSAP data remained close to constant, while the reference absorption varied about ±5 Mm^{-1} around the average, which is approximately the noise level of the absorption standard discussed above. When one type of aerosol is produced during an experiment, it is probable that ω_0 remains constant. In experiment 168_5, ω_0 was much more stable when calculated from the PSAP data than from the reference absorption, which supports the statement above (Figure 6).

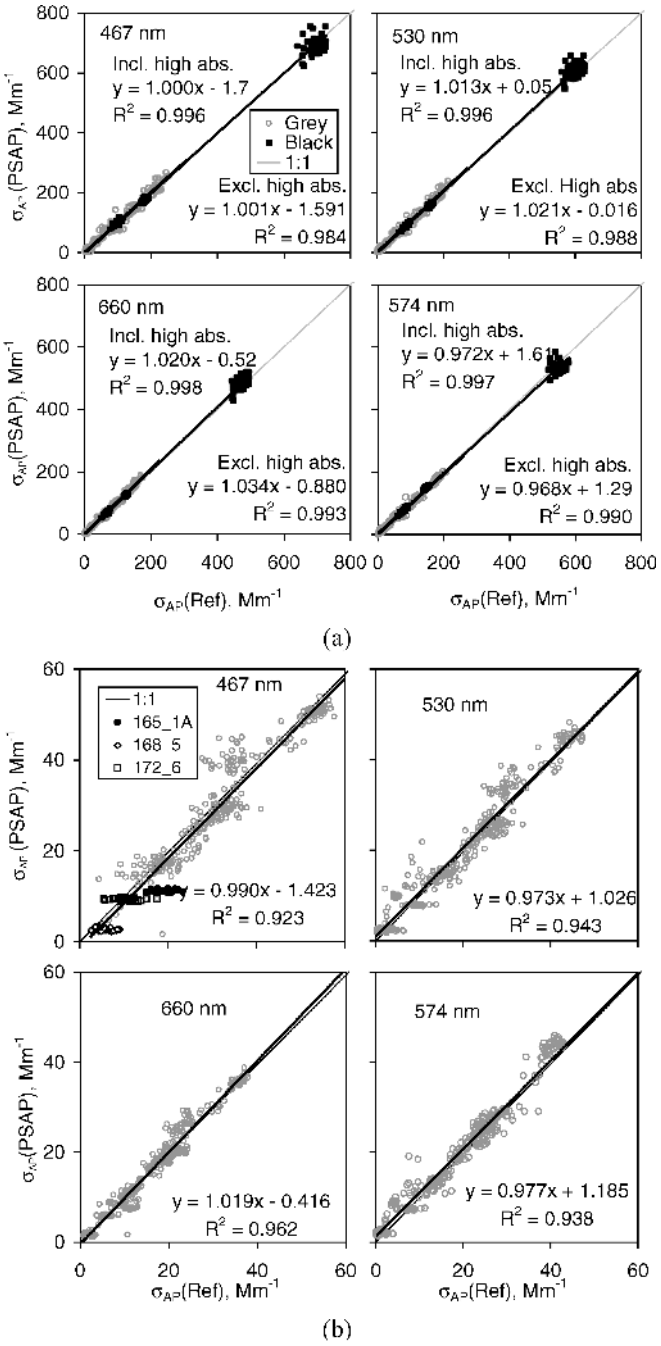

Figure 5. Comparison of the reference absorption coefficients and σ_{AP}(PSAP) = $(k_0 + k_1 h(\omega_0)\ln(Tr))\sigma_0 - s\sigma_{SP}$ after one iteration. The regression lines were fit for (a) all grey experiments and (b) experiments with σ_{AP}(467 nm) <60 Mm^{-1}.

A comparison of the linear regressions presented in Figures 2 and 5 shows the following:

1. Selecting the range of data resulted in significantly different slopes and offsets when using the Bond et al. (1999) formulas. For instance, for 530 nm the regression lines were σ_{AP}(PSAP) = $(0.85 \pm 0.02)\sigma_{AP}$(Ref) + (17.2 ± 2.4)

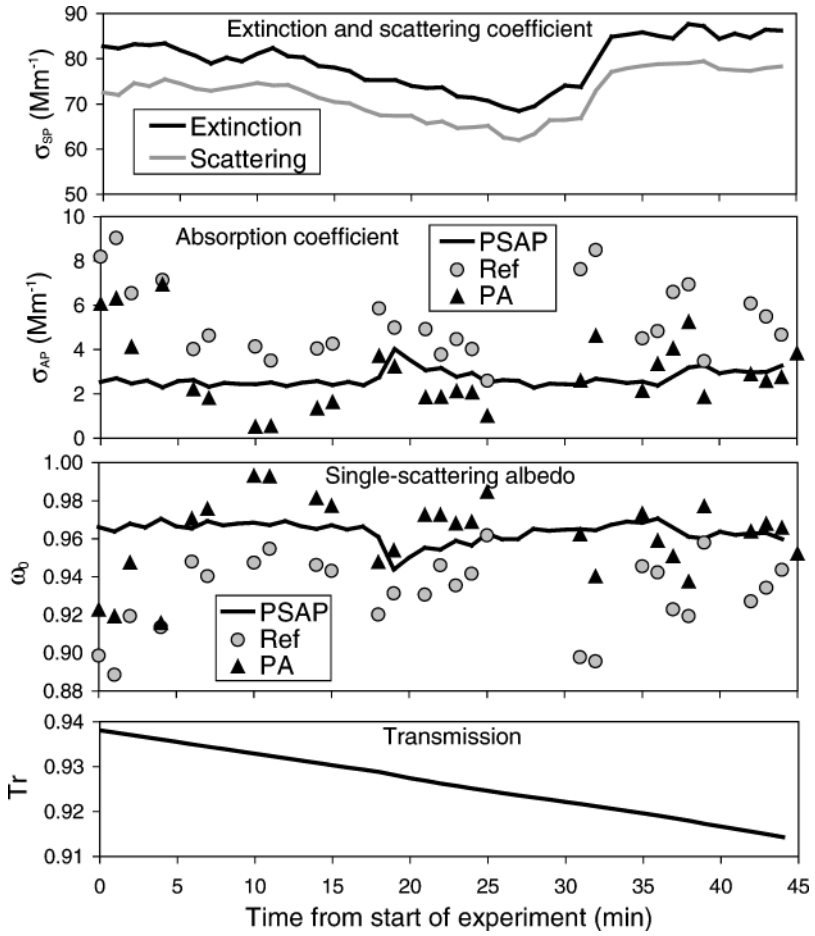

Figure 6. Experiment 168_5, data at $\lambda = 467$ nm.

Mm^{-1}, $\sigma_{AP}(PSAP) = (1.01 \pm 0.02)\sigma_{AP}(Ref) + (7.9 \pm 1.7)$ Mm^{-1}, and $\sigma_{AP}(PSAP) = (1.18 \pm 0.03)\sigma_{AP}(Ref) + (2.5 \pm 0.8)$ Mm^{-1} in the different data ranges in Figure 2. The error values are the 95% confidence limits. Using Equation (9) the slopes and offsets changed clearly less (Figure 5). For instance, for 530 nm the regression lineas were $\sigma_{AP}(PSAP) = (1.013 \pm 0.004)\sigma_{AP}(Ref) - (0.02 \pm 0.7)$ Mm^{-1}, $\sigma_{AP}(PSAP) = (1.021 \pm 0.008)\sigma_{AP}(Ref) + (0.05 \pm 0.7)$ Mm^{-1}, and $\sigma_{AP}(PSAP) = (0.973 \pm 0.025)\sigma_{AP}(Ref) + (1.03 \pm 0.6)$ Mm^{-1} in same data ranges as in Figure 2.

2. The goodness of the regression, as presented by R^2, increases significantly for regressions using the whole data, from about 0.95 using the Bond et al. (1999) formulas to about 0.997 using Equation (9), but it does not change significantly in the absorption range $\sigma_{AP}(467\text{ nm}) < 60$ Mm^{-1} (Figures 2 and 5).
3. For the nonmodified PSAP, the two methods yielded almost the same regression constants in the absorption range $\sigma_{AP}(467\text{ nm}) < 60$ Mm^{-1} (Figures 2b and 5b). The regression lines were $\sigma_{AP}(PSAP) = (1.036 \pm 0.020)\sigma_{AP}(Ref) + (2.45 \pm 0.44)$ Mm^{-1} and $\sigma_{AP}(PSAP) = (0.977 \pm 0.020)\sigma_{AP}(Ref) + (1.19 \pm 0.43)$ Mm^{-1} using the Bond et al. (1999) formulas and Equation (9). The error values are the 95% confidence limits for the slopes and offsets. The slopes and offsets do not overlap within the 95% confidence limits, so the two methods significantly differ statistically. However, the uncertainty of the reference absorption in the low absorption range is larger than the difference between the two algorithms. Therefore, in this range these data do not give unambiguous support for either method.

Apparent Absorption by Purely Scattering Aerosol

The transmission correction function was derived above using a constant scattering correction factors. If s were constant, using the right value of s in Equation (9) should yield zero absorption for white aerosol. However, a constant value does not work perfectly. Apparent absorption by white aerosols is a function of scattering coefficient, but this function also depends on the aerosol type: ammonium sulfate and polystyrene latex spheres (PSL) yield different apparent absorptions (Figure 7).

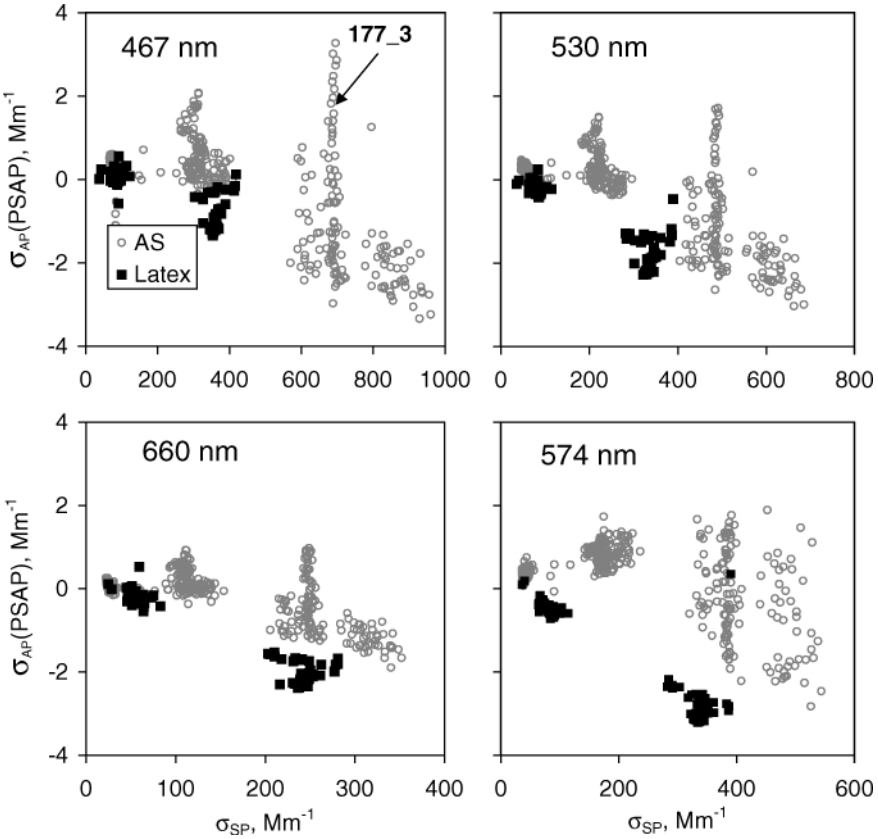

Figure 7. Apparent absorption in white aerosol experiments as a function of σ_{SP}.

A possible explanation is that the penetration depth of the particles to the filter material depends on particle size. The PSL particles' size distribution was more monodisperse (D_p = 0.5 μm) than that of the ammonium sulfate particles, produced using an ultrasonic humidifier (Sheridan et al. 2004). However, an explanation of this requires a theoretical treatment which is outside the scope of the present article. The apparent absorption is also a function of transmission (Figure 8), which suggests that Equation (9) should be changed further so that the scattering correction factor s would be a function of transmission, s = s(Tr). However, to keep the calculation procedure as simple as possible, only a range for s was estimated. The maximum s in each wavelength is the value that results in zero apparent absorption in the data point where σ_{AP}(PSAP)/σ_{SP} was largest and the minimum s is the value that results in zero apparent absorption in the data point where σ_{AP}(PSAP)/σ_{SP} was smallest. For instance, for λ = 530 nm the minimizing procedure yields s = 0.016, but the minimum and maximum values are 0.011 and 0.023 when using

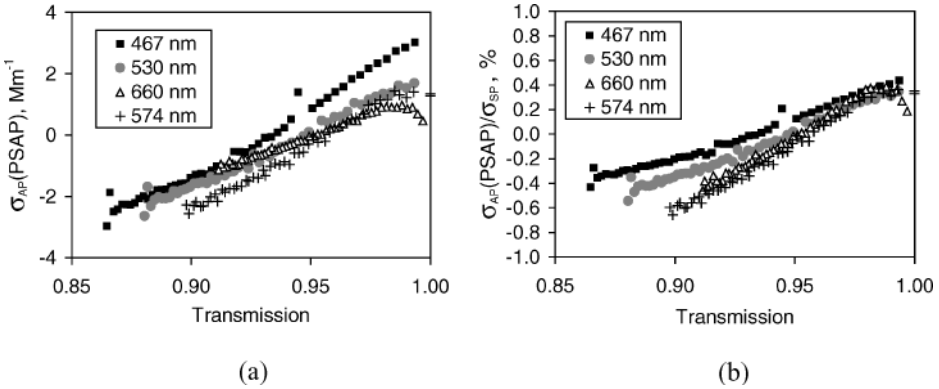

Figure 8. PSAP data from ammonium sulfate experiment 177_3. (a) Apparent absorption coefficient after using Equation (9) as a function of transmission. (b) Apparent-absorption-to-scattering-coefficient ratio, in %.

the k_0, k_1, h_0, and h_1 values presented in Table 3. The ranges of s for all wavelengths are presented in Table 3. The ratio of apparent absorption to scattering coefficient in experiment 177_3 was about ±0.5% (Figure 8b), which yields an uncertainty of approximately $\pm 0.005\ \sigma_{SP}$ to the absorption coefficient. In typical polluted air, scattering coefficients vary between 50 and 200 Mm^{-1}, so the uncertainty of absorption coefficient due to the uncertainty of s varies between ∼0.25 and 1 Mm^{-1}.

Wavelength Dependence of Absorption Coefficient of Laboratory-Generated Aerosol

The Ångstom exponent of the absorption coefficient α_{AP} was calculated from the 3λPSAP data between 467 and 660 nm. The average and 5th and 95th percentiles (in parentheses) of α_{AP}(PSAP) and α_{AP}(reference absorption) for the black aerosol experiments were 1.02 (0.94–1.17) and 1.09 (1.04–1.14), respectively. For the grey aerosol experiments at $\sigma_{AP} < 100\ Mm^{-1}$ the Ångström exponents were higher, 1.18 (0.96–1.42) and 1.29 (0.99–1.79), for the PSAP and the reference, respectively. The photoacoustic instrument alone yielded slightly lower values for the grey aerosols, 1.10 (0.58–1.43). For the grey aerosols the range of Ångström exponents was clearly the smallest, using the PSAP data (Figure 9b).

In the grey aerosol experiments the absorbing aerosol was the same, kerosene soot, as in the black aerosol experiments. Therefore α_{AP} should be the same for both types of experiments. This is the case for the average α_{AP}(PA), but not for α_{AP}(PSAP). This and the observation that α_{AP}(PSAP) decreases slightly with decreasing transmission, ∼0.1 from Tr = 1 to Tr = 0.7 (Figure 9b), show that the algorithm should still be improved. Possible ways would be, e.g., application of the Kubelka-Munk theory discussed above (section Basic formulas), or the two-stream radiative transfer model developed by Arnott et al. (2005) for the aethalometer.

ATMOSPHERIC AEROSOL EXPERIMENTS

RAOS Ambient Air Experiment

The first test of ambient aerosol measurements with the 3λPSAP was conducted during RAOS when most instruments

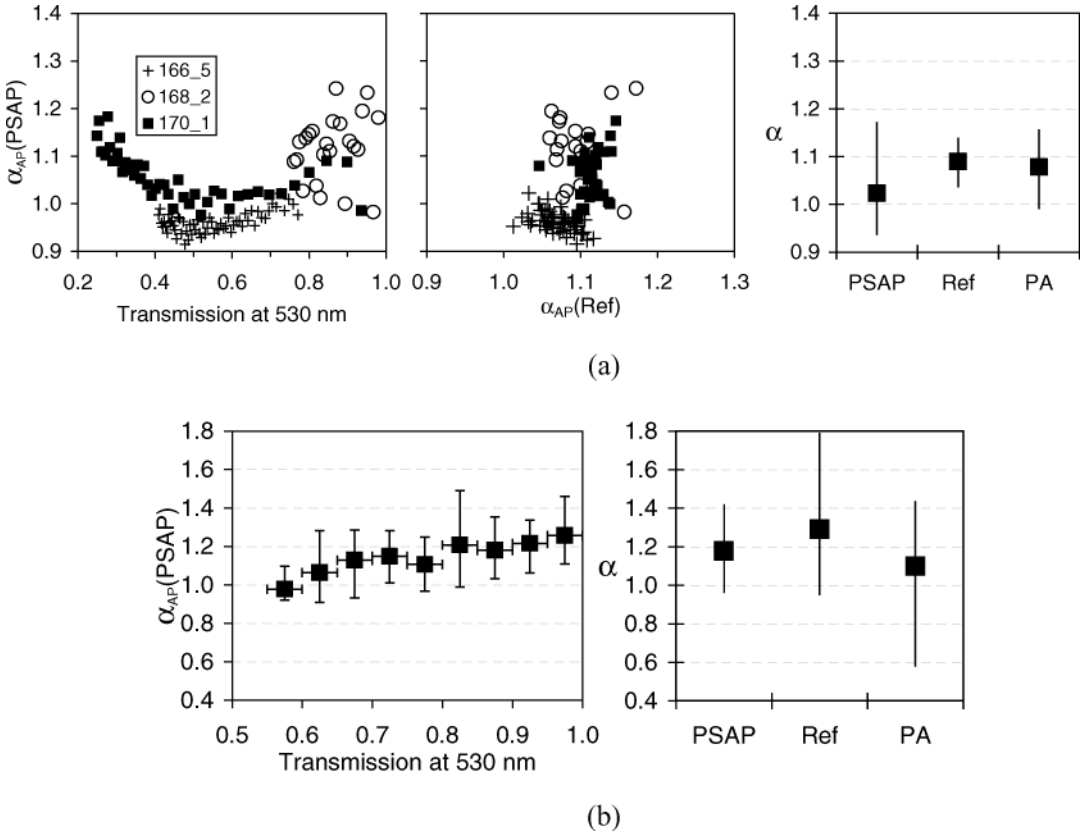

Figure 9. Ångström exponent of the absorption coefficient of laboratory-generated aerosol. (a) Black aerosol experiments. Left: α_{AP}(PSAP, 467–660 nm) as a function of transmision, all 1 min averages. Middle: α_{AP}(467–660 nm) of the reference absorption versus α_{AP}(PSAP), all 1 min averages. Right: average and range (5th and 95th percentiles) of α_{AP} using the PSAP, the reference, and the photoacoustic (PA) method. (b) Grey aerosol experiments at $\sigma_{AP} < 100\ Mm^{-1}$. Left: α_{AP}(PSAP, 467–660 nm) as a function of transmision, average and range (5th and 95th percentiles) in transmission intervals of 0.05. Right: average and range (5th and 95th percentiles) of α_{AP} using the PSAP, the reference, and the photoacoustic (PA) method.

were set for sampling ambient air over weekend, DOY 174–175.6 (day of the year in UTC), experiment 174_1. The OEC was not measuring, so reference absorption was provided by the photoacoustic instrument alone. The green scattering coefficient varied between ~10 and 25 Mm^{-1} and the absorption coefficient between ~0.5 and 5 Mm^{-1} before the high absoption peak on Monday morning at DOY ~175.6 (Figure 10).

It is apparent from the time series of the absorption coefficients that most of the time the absorption coefficients measured with the PSAP were slightly higher than those measured with the photoacoustic instrument (Figure 10). At $\lambda = 530$ nm the average difference $\Delta\sigma_{AP} = \sigma_{AP}(PSAP) - \sigma_{AP}(PA) = 0.6$ Mm^{-1}. A linear regression to all 1 min averaged data, including the high absorption peak, yields $\sigma_{AP}(PSAP) = 1.12 \times \sigma_{AP}(PA)$

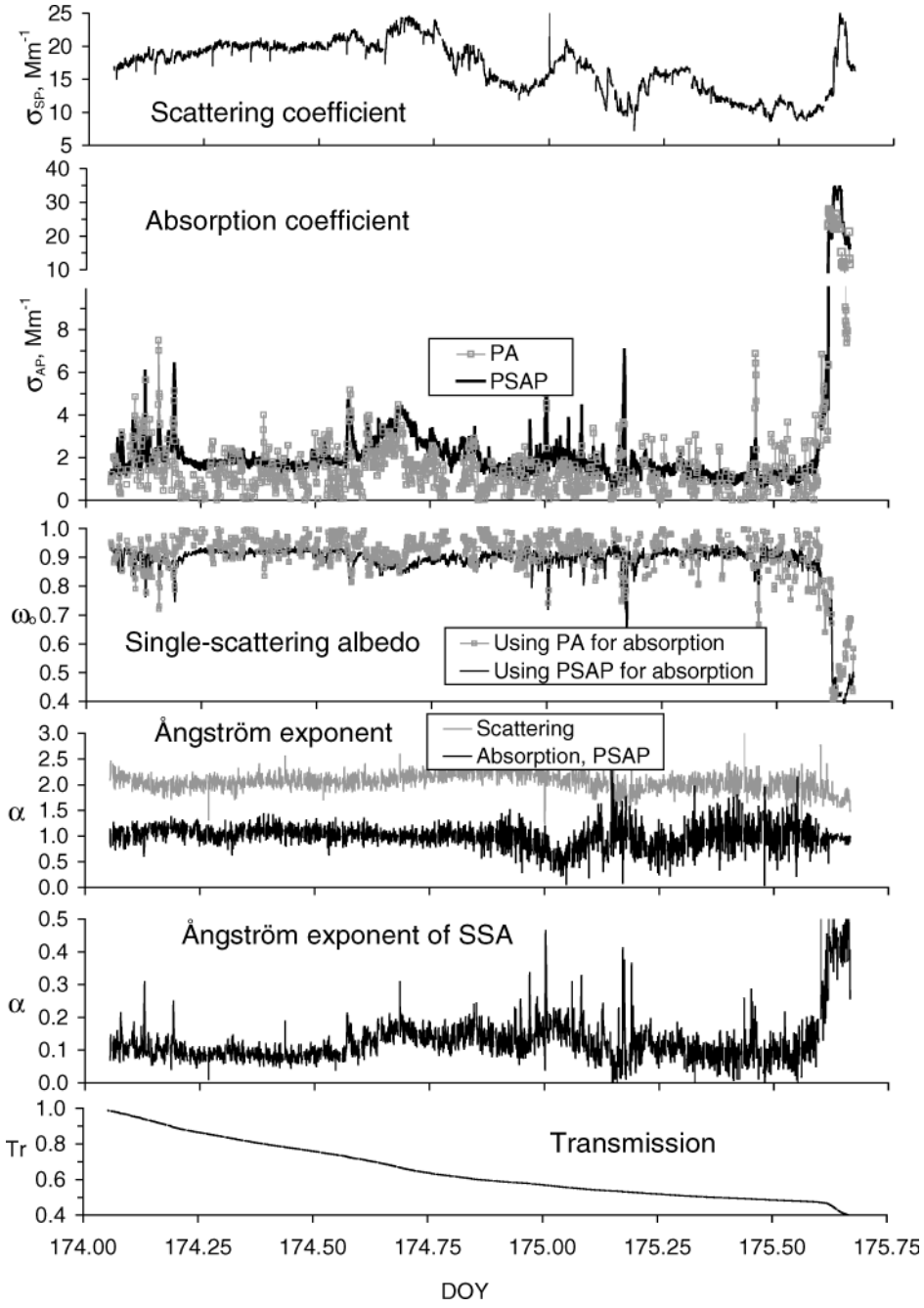

Figure 10. Scattering and absorption coefficients, Ångström exponents and transmission at $\lambda = 530$ nm during the RAOS ambient air experiment. The Ångström exponents were calculated from the scattering coefficients measured at 450 nm and 700 nm, and the absorption coefficients were measured at 467 nm and 660 nm.

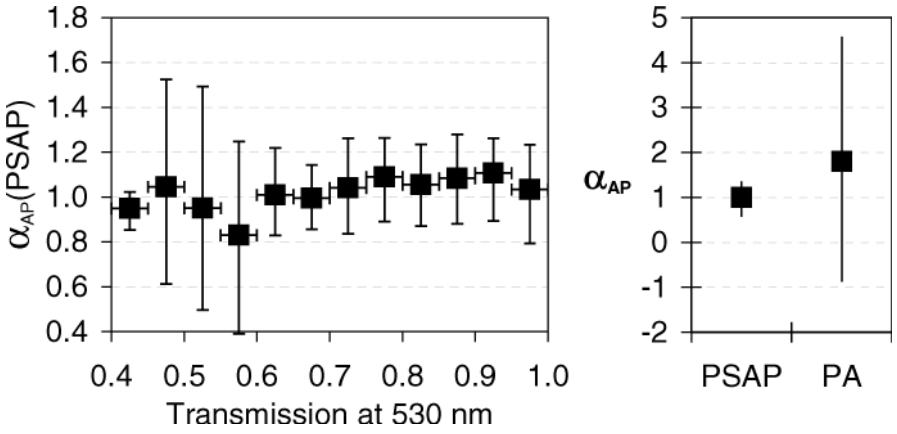

Figure 11. Ångström exponent of absorption coefficient during RAOS outdoor air experiment. Left: α_{AP}(PSAP) for wavelength range 467–660 nm as a function transmission. Right: average and 5th and 95th percentiles of α_{AP}(PSAP) for wavelength range 467–660 nm and α_{AP}(PA) for wavelength range 532–1047 nm.

$+ 0.5$ Mm^{-1}, $R^2 = 0.8$. However, if only those data points are considered where $\sigma_{AP}(PA) < 10$ Mm^{-1} and transmission was high (Tr > 0.7), the absorption coefficients were practically uncorrelated: the linear regression yields $\sigma_{AP}(PSAP) = 0.4 \times \sigma_{AP}(PA) + 1.8$ Mm^{-1}, $R^2 = 0.3$. The low correlation coefficient is most probably due to the noise of the photoacoustic instrument, which is supported by the observation that α_{AP}(PSAP) was almost constant compared with α_{AP}(PA) (Figure 11). The average (5th to 95th percentiles) of α_{AP}(PSAP) and α_{AP}(PA) were 1.00 (0.58–1.34) and 1.80 (−0.86–4.56), respectively. The wavelength dependence of single-scattering albedo was weaker than that of either scattering or absorption. The average Ångström exponent of ω_0, $\alpha(\omega_0)$, was 0.13 ± 0.07 over the whole outdoor air experiment and 0.10 ± 0.03 when Tr $>$ 0.7.

The 1λPSAP data were processed using the algorithm presented above and that presented by Bond et al. (1999). The absorption coefficients derived using these two methods agreed well for the RAOS ambient aerosol experiment data (Figure 12). The differences between these methods are large, with lower ω_0 and higher σ_{AP} as in the laboratory-generated aerosol experiments.

NEAQS

The second outdoor air experiment was conducted during the New England Air Quality Study (NEAQS) onboard the NOAA research vessel Ronald Brown in July–August 2002 (Quinn and Bates 2003). The cruise consisted of two legs, but only the second-leg data are discussed here. The instruments were used in a NOAA-PMEL measurement container together with a TSI 3λ Nephelometer and two 1λ PSAPs (Quinn et al. 2003; Bates et al. 2003). The absorption coefficients were calculated using the procedure described above. The 1λPSAP data were processed both with the 1λPSAP constants and with the 3λPSAP constants (k_0, k_1, s, g_0, and g_1) derived at RAOS. When using the 1λPSAP constants the 574 nm, absorption coefficients were about 16% higher than the 530 nm values. When using constants of the 3λPSAP interpolated to 574 nm, the 1λPSAP yielded about 2% higher values than at 530 nm Also, these 1λPSAP values are high or else the 3λPSAP values are too low, because $\sigma_{AP}(\lambda = 530$ nm) should be approximately 8% higher than $\sigma_{AP}(\lambda = 574$ nm), assuming $\alpha_{AP} = 1$. Bond et al. (1999) estimated that the unit-to-unit variability of the PSAPs is within ±6% of 95% confidence, so the difference of the 1λPSAP and the 3λPSAP at NEAQS is almost within these limits if the interpolated calibration constants are used for the 1λPSAP. It also has to be kept in mind that the spot diameters were determined with approximately 4% uncertainty, which results in approximately 8% uncertainty in the spot area and thus the absorption coefficients.

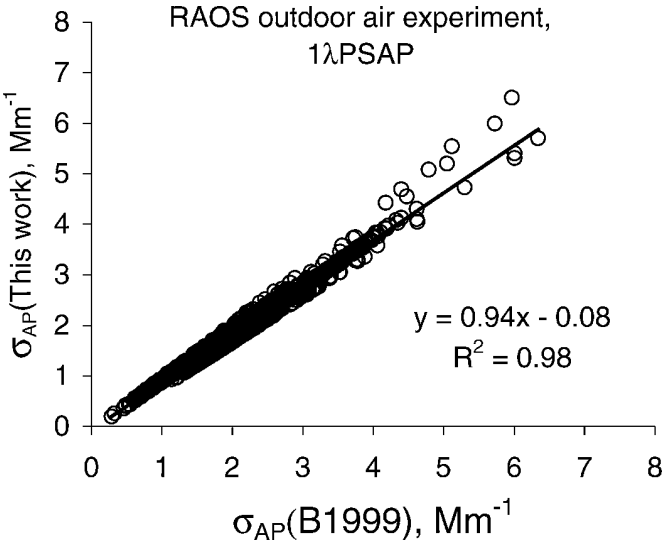

Figure 12. Absorption coefficient during RAOS outdoor experiment calculated from the 1λPSAP data using the method by Bond et al. (1999) and the method derived in this work.

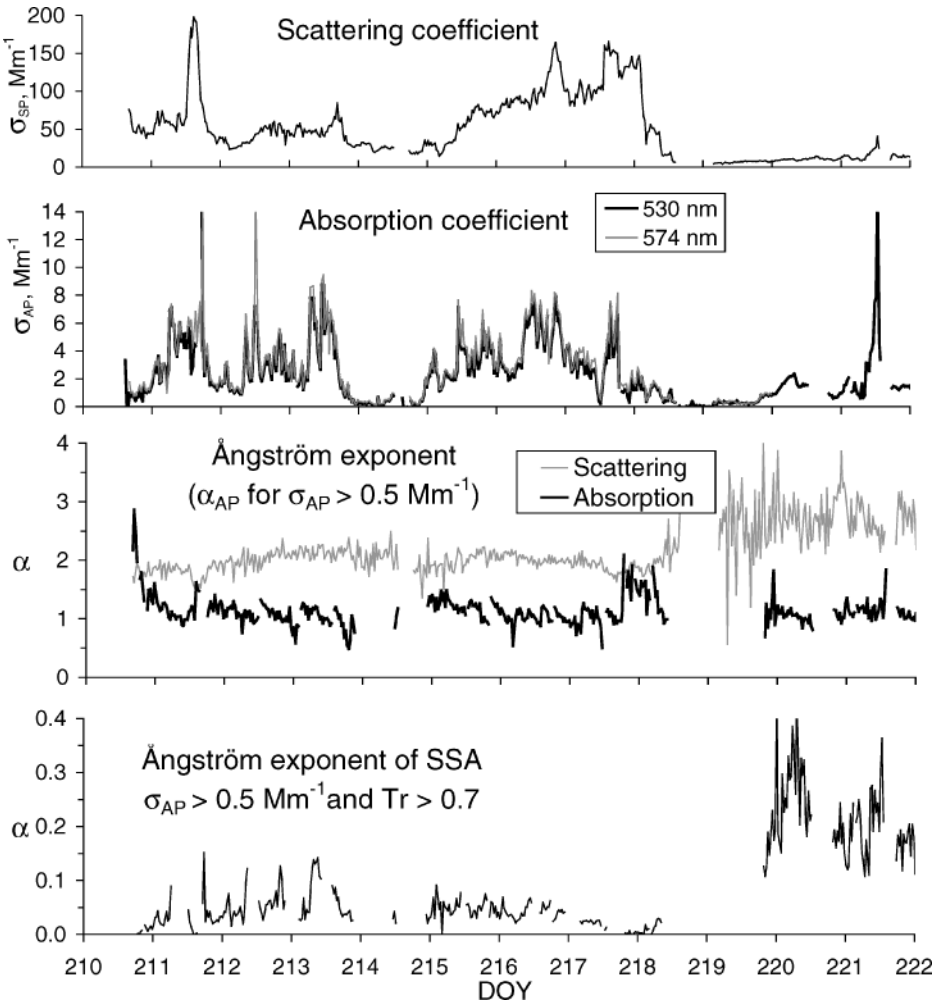

Figure 13. Submicron scattering and absorption data during NEAQS second leg. The presented scattering coefficient is at 530 nm.

Using the 3λPSAP and the nephelometer data, the Ångström exponents of scattering, absorption, and single-scattering albedo were calculated. Time series are shown in Figure 13. There was some variation of α_{AP} with transmission (Figure 14a), but at high transmissions it was was almost constant. For Tr > 0.8 and $\sigma_{AP} > 0.5$ Mm^{-1}, average α_{AP} (and 5th and 95th percentiles) was 1.19 (0.92–1.63). This is slightly higher than during the RAOS ambient air experiment, suggesting that the

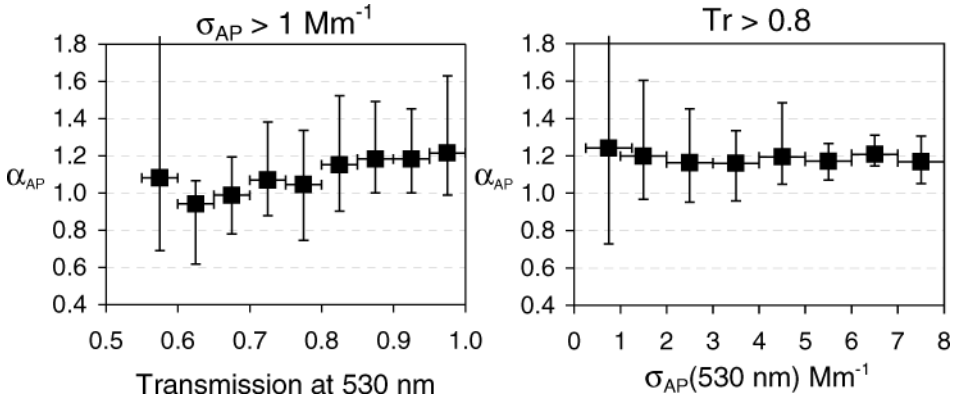

Figure 14. Ångström exponent of aerosol absorption coefficient for wavelength range 467–660 nm as a function transmission and absorption coefficient at $\lambda = 530$ nm during NEAQS second leg.

absorbing aerosol at these two locations were different. This is also supported by the different wavelength dependence of single-scattering albedo during NEAQS from that during the RAOS ambient air experiment. During NEAQS, $\alpha(\omega_0)$ varied from close to zero to about 0.4 (Figure 13). Before DOY 219 the average $\pm$ standard deviation of $\alpha(\omega_0)$ was 0.04 ± 0.04 and after DOY 219 0.22 ± 0.11.

SUMMARY AND CONCLUSIONS

A single-wavelength PSAP was modified to measure light absorption coefficient at three wavelengths. The main changes were adding a light source block and new detectors that work well for the whole wavelength range. The modified PSAP and an unmodified PSAP were calibrated against a reference absorption that was calculated as an average of two absorption standards, the difference between extinction and scattering coefficient, and a photoacoustic instrument.

The uncorrected absorption coefficients have to be multiplied by a transmission correction function that is a function of single-scattering albedo. This leads to a problem, because the absorption coefficient has to be known in order to calculate single-scattering albedo. This was solved by a simple iterative procedure that converges in one or two steps. The algorithm could still be improved, though. The Kubelka-Munk (KM) theory could be used as suggested by Lindberg et al. (1999) to find the best solution for the data processing. However, the use of the KM theory also requires information on the reflectance of the filter, which was not measured. An additional complication for the use of the KM theory would be that the filter material used in the PSAP consists of two layers, the reflectances of which are not equal.

The transmission correction functions and scattering correction factors reported here for the unmodified PSAP are different from those obtained by Bond et al. (1999), and there is no simple linear correction formula to change from one to the other. However, for typical atmospheric aerosol, such as the RAOS outdoor air experiment, these two methods differ only by about 6%. The results presented in this work were derived using quite a different absorbing aerosol than Bond et al. (1999), who used nigrosin, and still they are very close, which suggests that the absorption calibration does not significantly depend on the absorbing material. For the scattering correction factor, Bond et al. (1999) obtained a value $(0.02 \pm 0.02)/1.22 \approx 0.016 \pm 0.016$. The measurements in this work reduce the uncertainty of this factor. For instance, for the unmodified PSAP the factor was $\sim 0.023 \pm 0.006$. For the 3λPSAP the scattering correction factor increased with wavelength slightly but clearly, from ~ 0.013 at 467 nm to ~ 0.020 at 660 nm. This wavelength dependence is somewhat counterintuitive: shorter-wavelength light scatters more so the intuitive conclusion would be that the scattering correction factor should increase towards shorter wavelengths. It may have something to do with the cellulose background support structure of the filter material. This remains to be explained. The calibration factors depend on the filter material, so if other filter materials are used, a new calibration should be done.

The performance of the 3λPSAP in atmospheric aerosol measurements was tested both at RAOS and in a field experiment during New England Air Quality Study (NEAQS) onboard the NOAA research vessel Ronald Brown in July–August 2002. The absorption coefficients were calculated from the PSAP raw data using the transmission correction functions obtained from the laboratory experiment. The average Ångström exponent of absorption coefficient in the RAOS outdoor experiment was 1.00, but 1.18 at NEAQS. The spectral variation of ω_0 was used to distinguish aerosol types. The Ångström exponent of single-scattering albedo, $\alpha(\omega_0)$, at RAOS outdoor experiment was 0.10 ± 0.03 when transmission was >0.7. During NEAQS, average $\alpha(\omega_0)$ was 0.04 ± 0.03 during the first week of the second leg of the cruise and clearly higher, 0.22 ± 0.11, during the last two days of the cruise.

REFERENCES

Arnott, W. P., Moosmüller, H., Rogers, C. F., Jin, T., and Bruch, R. (1999). Photoacoustic Spectrometer for Measuring Light Absorption by Aerosol: Instrument Description, *Atmos. Environ*. 33:2845–2852.

Arnott, W. P., Moosmüller, H., Sheridan, P. J., Ogren, J. A., Raspet, R., Slaton, W. V., Hand, J. L., Kreidenweis, S. M., and Collett Jr., J. L. (2003). Photoacoustic and Filter-Based Ambient Aerosol Light Absorption Measurements: Instrument Comparisons and the Role of Relative Humidity, *J. Geophys. Res*. 108(D1):4034.

Arnott, W. P., Hamasha, K., Moosmüller, H., Sheridan, P. J., and Ogren, J. A. (2005) Towards Aerosol Light Absorption Measurements with a 7-wavelength Aethalometer: Evaluation with a Photoacoustic Instrument and 3 wavelength Nephelometer, *Aerosol Sci. Tech.* 39:17–29.

Bates, T. S., Quinn, P. K., Coffman, D. J., Covert, D. S., Miller, T. L., Johnson, J. E., Carmichael, G. R., Guazzotti, S. A., Sodeman, D. A., Prather, K. A., Rivera, M., Russell, L. M., and Merrill, J. T. (2004). Marine Boundary Layer Dust and Pollution Transport Associated with the Passage of a Frontal System over Eastern Asian, *J. Geophys. Res.*, 109, D19519, DOI: 10.1029/2003JD004094.

Bergstrom, R., Russell, P. B., and Hignett, P. (2002). Wavelength Dependence of the Absorption of Black Carbon Particles: Predictions and Results from the TARFOX Experiment and Implications for the Aerosol Single Scattering Albedo, *J. Atmos. Sci*. 59:567–577.

Bond, T. C. (2001). Spectral Dependence of Visible Light Absorption by Carbonaceous Particles Emitted from Coal Combustion, *Geophys. Res. Lett.* 28:4075–4078.

Bond, T. C., Anderson, T. L., and Campbell, D. (1999). Calibration and Intercomparison of Filter-Based Measurements of Visible Light Absorption by Aerosols, *Aer. Sci. Technol.* 30:582–600.

Bond, T. C., Covert, D. S., Kramlich, J. C., Larson, T. V., and Charlson, R. J. (2002). Primary Particle Emissions from Residential Coal Burning: Optical Properties and Size Distributions, *J. Geophys. Res.* 107(D21):8347.

Clarke, A. D. (1982). Effects of Filter Internal Reflection Coefficient of Light Absorption Measurements Made Using the Inegrating Plate Method, *Appl. Opti.* 21:3021–3031.

Clarke, A. D., Noone, K. J., Heintzenberg, J., Warren, S. G., and Covert, D. S. (1987). Aerosol Light Absorption Measurement Techniques: Analysis and Intercomparisons, *Atmos. Environ.* 21:1455–1465.

Gerber, H. E. (1982). Optical Techniques for the Measurement of Light Absorption by Particulates. In *Particulate Carbon, Atmospheric Life Cycle*, edited by G. T. Wolff and R. Klimisch. Plenum Press, New York, 145–158.

Hansen, A. D. A., Rosen, H., and Novakov, T. (1982). The Aethalometer—An Instrument for the Real-Time Measurement of Optical Absorption by Aerosol Particles, *Sci. Tot. Environ.* 36:191.

Heintzenberg, J., Charlson, R. J., Clarke, A. D., Liousse, C., Ramaswamy, V., Shine, K. P., Wendisch, M., and Helas, G. (1997). Measurements and Modelling of Aerosol Single-Scattering Albedo: Progress, Problems and Prospects, *Cont. Atmos. Phys*. 70:249–263.

Horvath, H. (1993). Atmospheric Light Absorption—A Review, *Atmos. Environ*. 27A:293–317.

Horvath, H. (1997). Experimental Calibration for Light Absorption Measurements Using the Integrating Plate Method—Summary of the Data, *J. Aerosol Sci.* 28:1149–1161.

Lin, C. L., Baker, M. B., and Charlson, R. J. (1973). Absorption Coefficient for Atmospheric Aerosols: A Method for Measurement, *Appl. Opt.* 12:1356–1363.

Lindberg, J. D., Douglass, R. E., and Garvey, D. M. (1993). Carbon and the Optical Properties of Atmospheric Dust, *Appl. Opt.* 32:6077–6081.

Lindberg, J. D., Douglass, R. E., and Garvey, D. M. (1999). Atmospheric Particulate Absorption and Black Carbon Measurement, *Appl. Opt.* 38:2369–2376.

Mukai, H., and Ambe, Y. (1986). Characterization of a Humic Acid–Like Brown Substance in Airborne Particulate Matter and Tentative Identification of its Origin, *Atmos. Environ*. 20:813–819.

Petzold A., Kramer H., and Schönlinner M. (2002). Continuous Measurement of Atmospheric Black Carbon Using a Multi-Angle Absorpton Photometer, *Environ. Sci. Pollut. Res.* 4:78–82

Petzold, A., and Schönlinner, M. (2004). Multi-Angle Absorption Photometry—A New Method for the Measurement of Aerosol Light Absorption and Atmospheric Black Carbon, *J. Aerosol Sci.* 35:421–441.

Petzold, A., Schloesser, H., Sheridan, P. J., Arnott, W. P., Ogren, J. A., and Virkkula, A. (2005). Evaluation of Multi-Angle Absorption Photometry for Measuring Aerosol Light Absorption, *Aerosol Sci. Technol.* 39:40–51.

Quinn, P. K., Coffman, D. J., Bates, T. S., Welton, E. J., Covert, D. S., Miller, T. L., Johnson, J. E., Maria, S., Russell, L., Arimoto, R., Carrico, C. M., Rood, M. J., and Anderson, J. (2003). Aerosol Optical Properties Measured Onboard the *Ronald H. Brown* During ACE Asia as a Function of Aerosol Chemical Composition and Source Region, *J. Geophys. Res.* submitted.

Quinn, P. K., and Bates, T. S. (2003). North American, Asian, and Indian Haze: Similar Regional Impacts on Climate? *Geophys. Res. Lett.* 30(11):1555.

Reid, J. S., Hobbs, P. V., Liousse, C., Vanderlei Martins, J., Weiss, R. E., and Eck, T. F. (1998). Comparisons of Techniques for Measuring Shortwave Absorption and Black Carbon Content of Aerosols from Biomass Burning in Brazil, *J. Geophys. Res.* 103:32031–32040.

Schnaiter, M., Horvath, H., Möhler, O., Naumann, K.-H., Saathoff, H., and Schöck, O. W. (2003). UV-VIS-NIR Spectral Optical Properties of Soot and Soot-Containing Aerosols, *J. Aerosol Sci.* 34:1421–1444.

Sheridan, P. J., Arnott, W. P., Ogren, J. A., Andrews, E, Atkinson, D. B., Covert, D, Moosmüller, H., Petzold, A., Schmid, B., Strawa, A. W., Varma, R., and Virkkula, A. (2005). The Reno Aerosol Optics Study: An Evaluation of Aerosol Absorption Measurement Methods, *Aerosol Sci. Technol.* 39:1–16.

Van de Hulst, H. C. (1957) *Light Scattering by Small Particles*. Wiley, New York. 1957.

Virkkula, A., Ahquist, N., Covert, D., Sheridan, P., Arnott, W. P., Ogren, J. (2005). A Three-wavelength Optical Extinction Cell for Measuring Aerosol Light Extinction and its Application to Determining Light Absorption Coefficient, *Aerosol Sci. Technol.* 39:52–67.

Weingartner, E., Saathoff, H., Schnaiter, M., Streit, N., Bitnar, B., and Baltensperger, U. (2003) Absorption of Light by Soot Particles: Determination of the Absorption Coefficient by Means of Aethalometers, *J. Aerosol Sci.* 34:1445–1463.

Weiss, R. E. and Waggoner, A. P. (1984). Aerosol Optical Absorption: Accuracy of Filter Measurement by Comparison with in-situ Extinction, In: *Aerosols*, edited by B. Y. H. Liu, D. Y. H. Pui, and H. Fissan. Elsevier, New York, Amsterdam, Oxford, 397–400.